Radiation Dosages for NdFeB Magnets in CBETA

Joseph Petrullo[*] and Nilanjan Banerjee[†]

Cornell University

This paper creates models of various components of CBETA and conducts simulations of electron beam irradiation to calculate dose rates on NdFeB permanent magnets. Using Geant4 simulation software, two models were created which fired 42MeV beams and measured the resulting dosage of radiation on nearby permanent magnets. In the first model, the beam was incident on a viewscreen, and the maximum dose rate obtained on a nearby magnet was .97±.0007 Gy/μC which corresponds to 1910±3 hrs of continuous operation at a beam current of 150 pA, if the maximum allowed dose is 1 kGy. The second model is of a splitter section, and the results indicate that radiation dose rate increases as a function of the incident angle as the beam enters the 42MeV chamber line. In Model II, a half-quadrupole magnet experienced the highest dose rate at 0.0909±.0005 Gy/μC, corresponding to 20,400±140 hrs of operation at 150 pA until the magnet reaches a dose of 1 kGy. For this second model, it was also observed that vertical momenta proportionally decrease radiation dosage on the magnets.

I. INTRODUCTION

In particle accelerators, high-energy electron beam radiation has proven to be damaging to NdFeB permanent magnets on which many accelerators rely. At Brookhaven National Laboratory, radiation demagnetization has prompted investigations into more resistant magnets for applications such as insertion devices (IDs) in the National Synchroton Light Source II. In one study at BNL, electron beam irradiation caused an 85% decrease in the magnetic intensity of NdFeB magnets after an absorbed dose of $5 \cdot 10^5$ Gray[1]. These permanent magnets were used in rotary ferrofluidic feedthroughs and synchroton IDs, which would suffer a serious degradation in performance as a result of irradiation. Though, annular NdFeB magnets had shown resistance to demagnetization due to the absence of a stronger demagnetizing field that would have otherwise been present in a disk-shaped magnet. A similar experiment was conducted at Cornell's CLASSE facilities. Demagnetization of NdFeB magnets used in IDs was observed to be a function of radiation dose, demagnetizing temperature, and orientation of the material's magnetic field[2].

In collaboration with BNL, Cornell physicists have been constructing a prototype Energy Recovery Linac known as CBETA. At CBETA, electron beams will be recirculated around the accelerator and return their energy to superconducting cavities. This test accelerator is heavily reliant on NdFeB magnets, especially in its return loop. Thus, investigating radiation demagnetization is critical to ensure CBETA's long-term functionality. In CBETA, electron beams will often make contact with viewscreen detectors and experience beam loss. Thus, the primary motivation for this paper is to contribute to studies of NdFeB demagnetization pertaining to CBETA by simulating various sources of beam irradiation. In this

paper, there are two distinct models: one in which an electron beam makes contact with a viewscreen, and another which models a splitter section immediately prior to entering the return loop. Both of these models were implemented and tested in a particle simulation software known as Geant4.

II. GEANT4 SIMULATION SOFTWARE

Geant4, developed by CERN, is a C++ toolkit used for simulating the passage of particles through matter. Its usage spans a broad range of applications in sub-fields such as nuclear, high energy, and accelerator physics as well as medical and space sciences. Geant4's Monte Carlo simulation software has been shown to accurately demonstrate particle-matter interactions[3]. This paper utilizes Geant4 to simulate irradiation of a high-energy electron beam and analyze the resulting dosages of radiation on NdFeB permanent magnets. The models in this paper were approximations of relevant components implemented in a geometry class supported by Geant4. Some of the more advanced geometries were implemented through the conversion of CAD files to GDML, or Geometry Detector Markup Language, which allows complex tessellations to be implemented in a Geant4 geometry class. This paper uses InStep V2 Software[4] which supports the conversion of various file types, such as STL/STEP to GDML. Additionally, this paper uses the QBBC physics list for simulating events, which is worth noting as these lists describe the physical processes which particles will obey.

In Geant4, 42 MeV electron beams were modeled as gaussian particle sources to be scattered in various scenarios, depositing radiation on nearby NdFeB magnets. Radiation dose rates on the magnets were then calculated using scoring volumes, which "score" particles passing through a volume and calculate the resulting energy deposited. The total deposited energy in eV was then converted to radiation dose rate in units of Gy/μC. The first model, as outlined in the next section, simulates an electron beam hitting a stainless steel viewscreen.

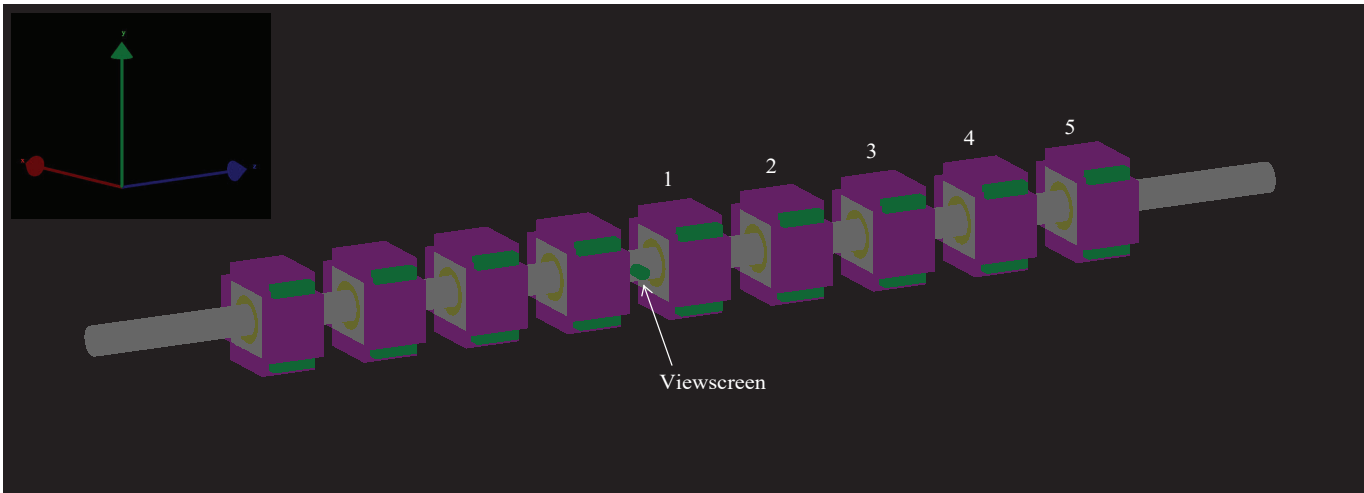[*] jgp98@cornell.edu
[†] nb522@cornell.edu

Figure 1: Beam pipe, surrounding magnets, and viewscreen. The electron beam is incident from the left end of the pipe, and magnets 1 - 5 are to be dosed for radiation.
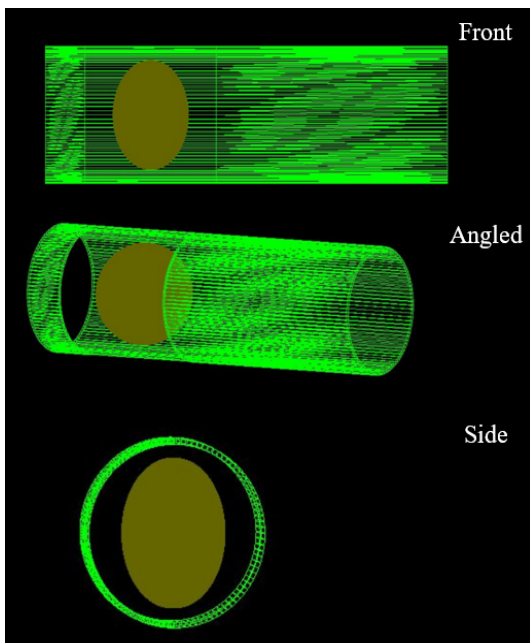

Figure 2: Beryllium Oxide Viewscreen (brown) and Viewscreen Case (green).

III. MODEL I: BEAM HITTING VIEWSCREEN IN STRAIGHT-SECTION

A. Geometry

The first model consists of a perfectly straight aluminum beam pipe of 3 meters in length with inner and outer radii of 35 mm and 38 mm, respectively. Additionally, the beam pipe was surrounded by 9 evenly spaced FFA magnets comprised of NdFeB material enveloped by an iron/aluminum frame and copper coils as shown in Figure 1. The NdFeB magnet material to be dosed was modeled as a hollow cylinder. Using a density of approximately 7700 kg/m^3 for NdFeB, the mass of each permanent magnet was estimated to be 5.62 kg. Within the beam pipe, a model of a viewscreen and its surrounding case were placed 13 cm in front of Magnet 1 which was centered at the beam pipe's origin. The solid BeO viewscreen disk was rotated 45 degrees about the vertical axis as to direct the beam along the central axis of the stainless-steel viewscreen case (Figure 2). Furthermore, a 42 MeV electron beam incident from the left end of the beam pipe was directed such that it would make contact with the viewscreen and its case. With back-scattering unlikely, the scattered particles mainly hit the FFA structures which are located past the point of the viewscreen (numbered 1 through 5 in Figure 1). Thus, dose rate calculations were performed only on these magnets.

B. Benchmarking

This paper utilized a benchmarking technique to ensure that each model had simulated a high enough number of events such that the dose rate in Gy/μC did not significantly depend on the number of simulated particles. This technique was performed by measuring radiation dose rate as a function of the number of simulated events, plotting the distribution, and selecting a number of events which experiences a convergence significant enough to ensure that the dose rate calculations were not heavily impacted by the amount of simulated particles. In Figure 4, the benchmarking distribution for Model I is given as an example, where 1 million events was chosen as a benchmark to calculate average dose rates. This process was repeated for both Model I and Model II.
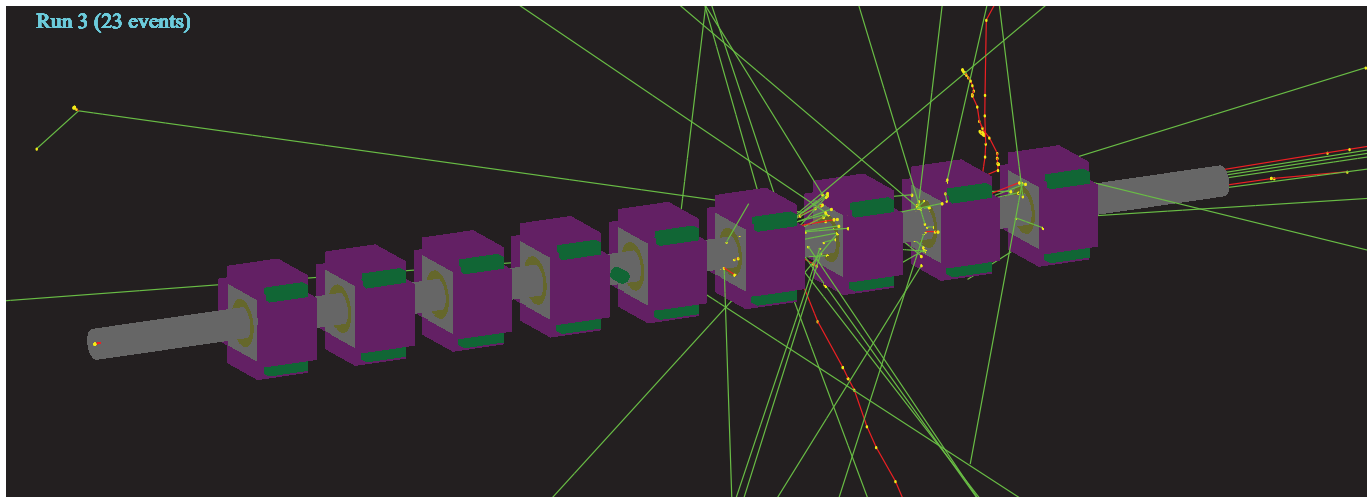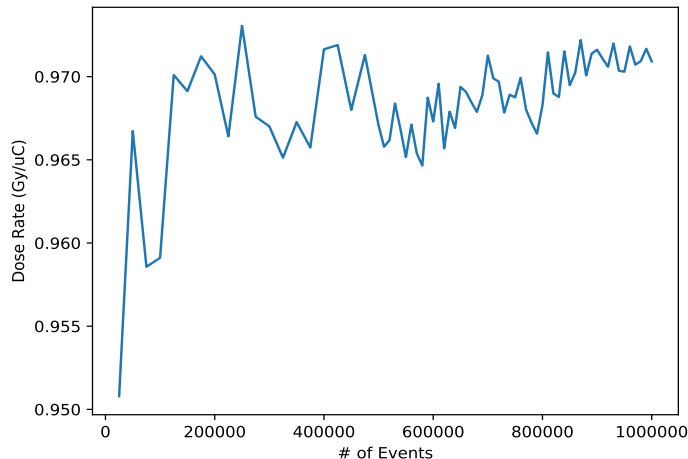
Figure 3: Model 1 Scattering Shower
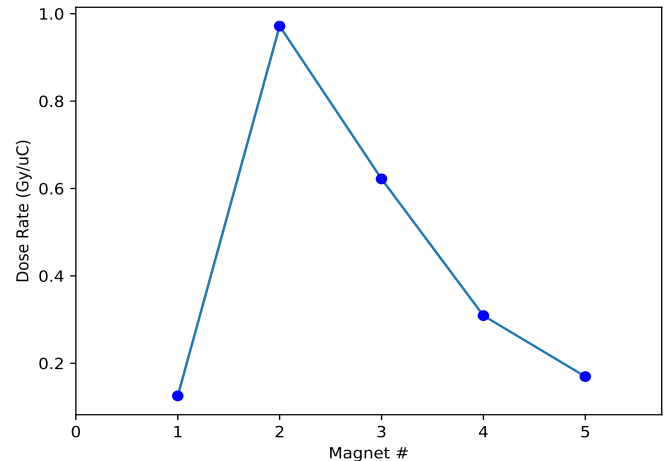

Figure 4: Model I Benchmarking Distribution

Figure 5: Model I Average Dose Rate per Magnet

C. Results

As previously stated, the five permanent magnets appearing past the point of the viewscreen were dosed, and the results are plotted above in Figure 5. Additionally, average dose rates were calculated over 10 independent runs for each magnet. Evidently, the magnet immediately beyond the viewscreen receives the smallest dosage of radiation. The second magnet receives the highest dosage, after which the dose rate decreases rapidly as each subsequent magnet is further from the viewscreen case. An image of the resulting scattering shower is also provided (Figure 3).

At CBETA, the estimated limit for radiation dosage is 1 kGy to ensure the accelerator's long-run functionality. Using the maximum dose rate per unit coulomb from Magnet 2 at .97±.0007 Gy/μC, and a desired beam current of 150 pA, the magnet can sustain 1910 continuous hours of operation before reaching a total absorbed dose of 1 kGy.

IV. MODEL II: TOTAL BEAM LOSS IN SPLITTER SECTION

A. Geometry

In Model II, the geometry is much more extensive, again featuring an aluminum accelerator pipe with 35 and 38 mm radii, now with a radius of curvature of 5.6642 m. The surrounding FFAs are grouped in pairs with the exception of Magnet 1, the half-quadrupole, as shown in Figure 6. The model also contains approximations of a stainless steel gate valve and several flanges. Though,
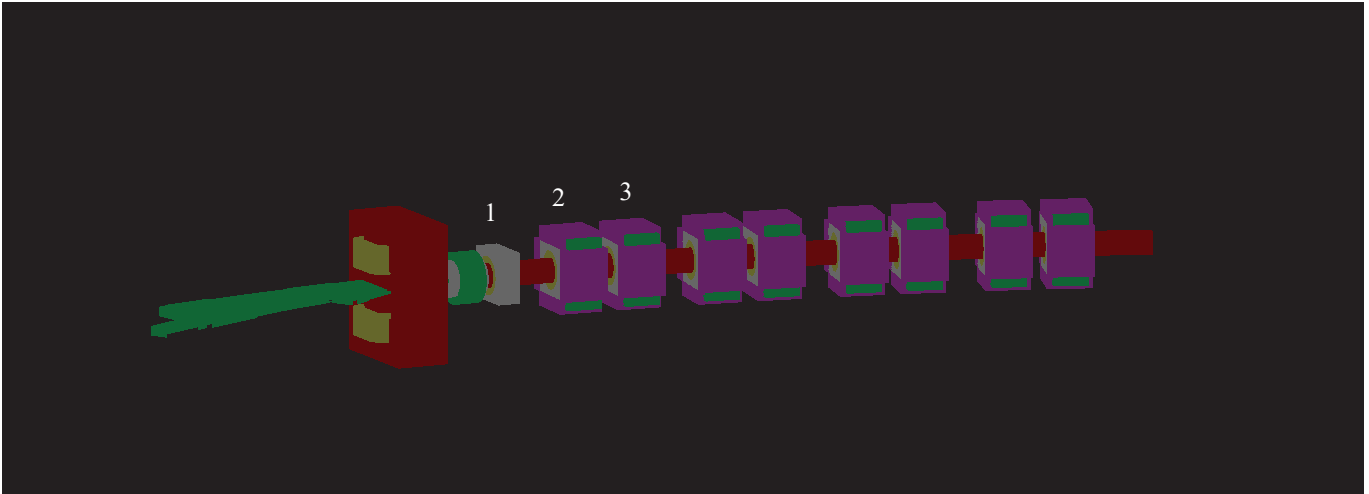
Figure 6: Model II geometry, note that the first FFA is not fully encased, and is the half-quadrupole magnet.
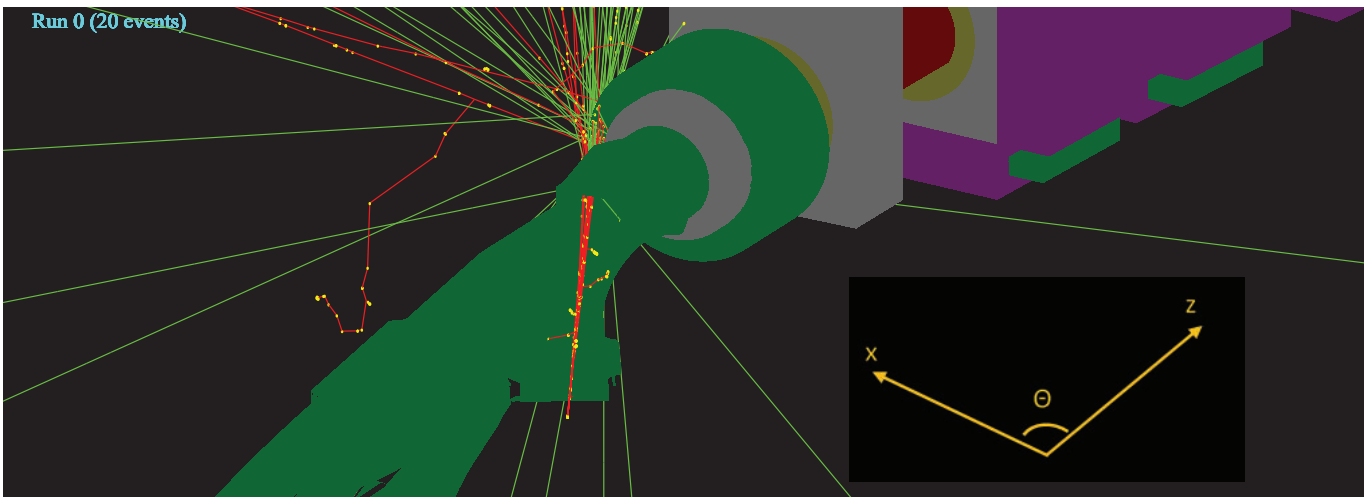

Figure 7: Electron beam in the 42 MeV line of the beam chamber. Note that the electromagnet and top portion of the beam chamber are omitted to provide a clear view of the beam's trajectory.
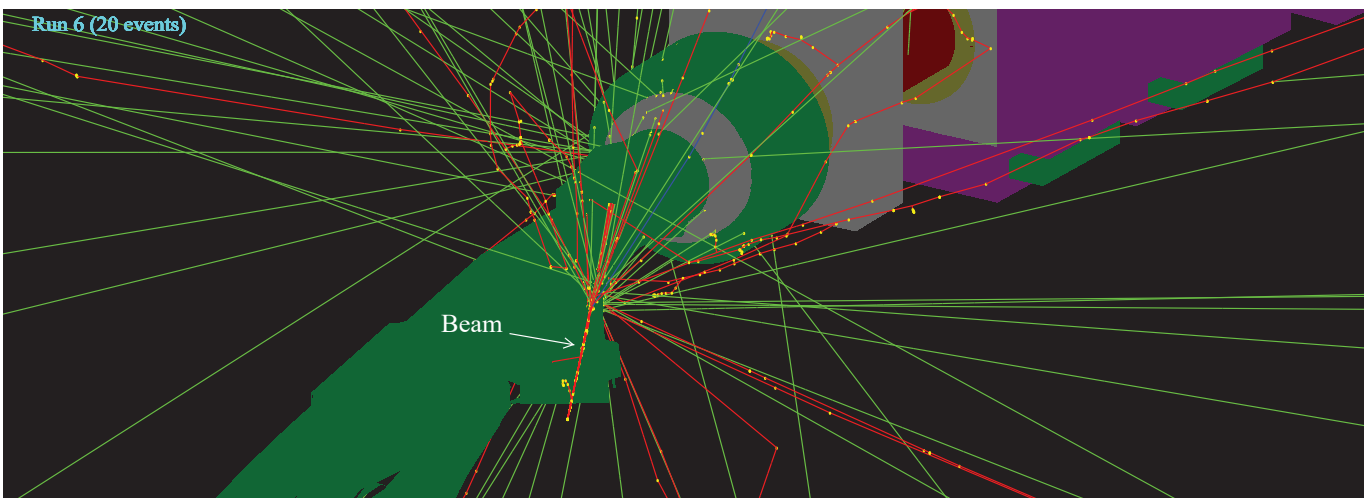

Figure 8: Scattering shower produced by incident angles greater than 60°, where the beam hits the right inner wall of the chamber.

the main features of this model are a beam splitter and chamber that the beam will travel through as it enters the 42 MeV line.

B.   Electron Beam in 42 MeV Line

For Model II, a 42 MeV beam is incident from inside the rightmost chamber section as shown in Figures 7 and 8, where it is shot from various angles with respect to the xz-axis. The resulting dose rates on Magnet 1 as a function of the incident angle are shown in Figure 9 below.
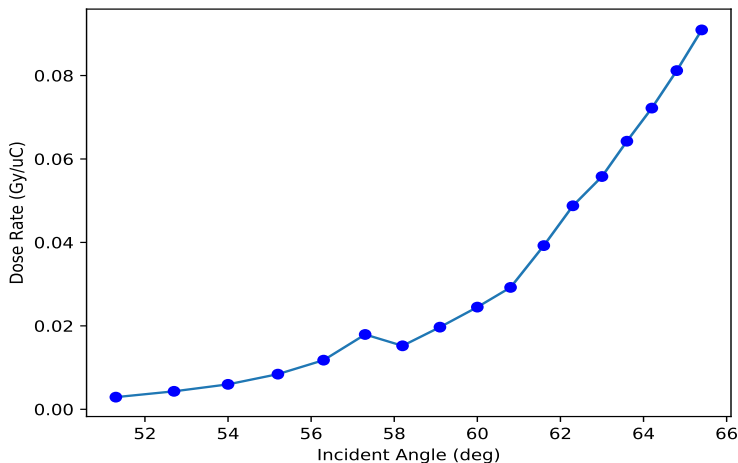
C.   Results

Figure 9: Radiation Dose Rate on Magnet 1 vs. Incident Angle

The positive correlation between the angles in range 51.3°-60° and radiation dose rate on Magnet 1 is clear: as the angle increases, the beam travels further into the beam splitter and is closer in distance and direction to Magnet 1, therefore it is more likely that particles will hit the permanent magnet material. Though, at incident angles greater than 60 degrees, the beam instead hits the right wall of the beam chamber and scatters more severely. Yet the more erratic scattering shower produced from hitting the right inner wall of the beam chamber also corresponds to higher dosages of radiation on Magnet 1. Even after the beam begins to hit the chamber's inner wall, radiation dose rate continues to increase as a function of the incident angle.

The highest dose rate on Magnet 1 was observed at an incident angle of 65.4°. This rate of 0.0909±.0005 Gy/μC corresponds to 20,400±140 hrs of operation at a beam current of 150 pA before reaching the 1 kGy dose limit. However, in the best case scenario with a dose rate of .0029 Gy/μC, Magnet 1 reaches 100,000 hours

of operation at a maximum beam current of 309 pA. Dose rates on Magnet 2 and Magnet 3 obey the same relationship as Magnet 1 regarding angle of incidence. However, the maximum dose rates on these subsequent magnets are much smaller. The max dose rates on Magnets 2 and 3, similarly observed at the largest angle 65.4°, are 0.009±.0003 and 0.0019±.0001 Gy/μC, respectively. Thus, Magnet 1 experiences a higher dose rate by a factor of 10 or 100 in comparison to Magnets 2 and 3, making it the most likely to suffer from demagnetization effects. For Magnets 2 and 3, both of which easily reach 100,000 hrs of operation, can do so with maximum beam currents of 309±10 pA and 1.46±.08 nA, respectively.

Some additional data was recorded for the beam with incident angles of 64.2°, 64.8°, and 65.4°. At such incident angles with respect to the xz-plane, the beam was also given slight vertical momenta (represented by an angle with respect to the xy-plane) to investigate the possibility of radiation dose rates increasing as the beam fanned away from a perfectly horizontal trajectory. The results are shown below in Table 1, where the leftmost column is the vertical angle with respect to the xy-plane, and the remaining columns illustrate how the dose rate changes for three incident angles in the xz-plane as the beam is given various vertical momenta.

TABLE I

Vertical Angle	64.2°(xz)	64.8°(xz)	65.4°(xz)
-5.7°	0.052	0.059	0.066
-2.9°	0.065	0.073	0.082
0°	0.072	0.081	0.091
2.9°	0.066	0.074	0.083
5.7°	0.054	0.060	0.067

Evidently, for the angle range 64.2°-65.4°, radiation dose rates decrease symmetrically as the beam is given either positive or negative vertical momenta. This was the expected result as the scattered particles are less likely to hit Magnet 1 if given a substantial vertical trajectory. The simulations performed with this second model illustrate that regarding the electron beam, favorable angles exist such that the radiation dose rate on nearby NdFeB magnets are minimized.

V.   CONCLUSION

Ultimately, the simulations performed for each model provide two distinct outlooks on minimizing radiation demagnetization in CBETA's permanent magnets. Regarding Model I, the electron beam must come into contact with viewscreens as it travels around the accelerator loop. This inevitability limits the available options to minimize radiation dosage on surrounding magnets.

However, Model II provides a more optimistic outlook. In situations similar to Model II, the electron beam can be directed at angles which are more favorable for limiting radiation dosage and thus protecting the strength of the permanent magnets. In the near future, it is critical to conduct additional simulations of other scenarios. For example, back-scattering effects of the radiation shielding wall which surrounds the accelerator could provide valuable insight as to how the wall contributes to radiation dosages. Therefore, this paper's discussion of dose rates on CBETA's permanent magnets prompts further investigation.

[1] N. Simos, S. Ozaki, N. Mokhov, A. Zeller, W. Mittig, and F. Pellemoine, Demagnetization of nd2fe14b, pr2fe14b, and sm2co17 permanent magnets in spallation irradiation fields, 10.1109/TMAG.2017.2769040.

[2] A. Temnykh, Measurement of permanent magnet material demagnetization due to irradiation by high energy electrons, in *2007 IEEE Particle Accelerator Conference (PAC)* (2007) pp. 1230–1232.

[3] S. Agostinelli, J. Allison, and K. Amako, *Nuclear Instruments and Methods in Physics Research Section A: Accelerators, Spectrometers, Detectors and Associated Equipment*, Vol. 506 (2003) pp. 250–303.

[4] https://www.solveering.com/InStep/instep.aspx.